FOREX Publication
Open Access | Rapid and quality publishing

International Journal of
Electrical and Electronics Research (IJEER)
Research Article | Volume 13, Issue 4 | Pages 784-791 | e-ISSN: 2347-470X

GA-Optimized FACT-SMES Coordination and APF Selection for Enhanced AGC Stability in Deregulated Hybrid Power Systems

Sunil Kumar[1*], Prof (Dr) SK Gupta[2]

[1]*Department of Electrical Engineer, PHD Scholar DCRUST Murthal, Sonipat, Haryana, India; Email: 18001902906sunil@dcrustm.org*
[2]*Department of Electrical Engineer, Professor, DCRUST, Murthal, Sonipat, Haryana, India; Emai: drskgupta.ee@dcrustm.org*

***Correspondence:** *Sunil Kumar; Email: drskgupta.ee@dcrustm.org*

ABSTRACT- This research investigates the enhancement of frequency stability in a hybrid power system operating under deregulated conditions. The study integrates Flexible AC Transmission System (FACT) devices including SSSC, UPFC, TCPS, and TCSC with Superconducting Magnetic Energy Storage (SMES) units, optimized using Genetic Algorithms (GA). PID and PIDF controllers are employed for frequency regulation, and their performance is evaluated through various case studies. Results demonstrate that the combination of FACT devices with SMES, tuned via GA, significantly improves dynamic response, reducing settling time and peak overshoot. Among the FACT devices, UPFC and SSSC exhibit superior performance, while the CPI-PDF controller provides the best damping effect. The use of PIDF with SSSC+SMES gives 4.92s settling time. The findings highlight the effectiveness of intelligent optimization techniques in enhancing power system stability, with SMES contributing to a 32% faster settling time and a 54% reduction in overshoot. The study provides practical recommendations for controller and device selection based on specific grid requirements, offering valuable insights for modern power systems with high renewable energy penetration. The entire system is simulated using MATLAB 2026a Simulink.

General Terms: Automatic Generation Controller, Load Frequency Control, Proportional Integral Derivative, Genetic Algorithm et. al.
Keywords: Hybrid power system, FACT devices, SMES, Genetic Algorithm, Frequency stability, PIDF control.

ARTICLE INFORMATION
Author(s): Sunil Kumar, and Prof (Dr) SK Gupta;
Received: 24/08/2025; **Accepted:** 26/11/2025; **Published:** 15/12/2025;
E- ISSN: 2347-470X;
Paper Id: IJEER 2408A18;
Citation: 10.37391/ijeer.130418
Webpage-link:
https://ijeer.forexjournal.co.in/archive/volume-13/ijeer-130418.html
Publisher's Note: FOREX Publication stays neutral with regard to jurisdictional claims in Published maps and institutional affiliations.

1. INTRODUCTION
The deregulation of power systems has introduced challenges in maintaining frequency stability due to fluctuating loads and decentralized control. Renewable energy integration further complicates grid stability, necessitating advanced control mechanisms. FACT devices and energy storage systems like SMES offer dynamic compensation, while intelligent tuning methods such as Genetic Algorithms (GA) optimize controller performance.

This study focuses on:
- Modeling a two-area hybrid power system with AVR and FACT devices [1,4,7 & 8].
- Integrating SMES for energy storage and transient support [8 & 9].
- Optimizing PID/PIDF controllers using GA [2 & 3].
- Evaluating performance under different configurations [14].

1.1. Background and Motivation
Deregulation has fragmented control authority, increased renewable penetration, and introduced bidirectional power flows, severely challenging Load Frequency Control (LFC). Traditional PI/PID controllers fail under high uncertainty. FACT devices and energy storage are essential for dynamic support.

1.2. Literature Review

Ref Key	Contribution
Arya (2021) [1]	GA-tuned PID for thermal-hydro-gas system
Chandrashekar (2019) [4]	AVR + TCSC in deregulated system
Deepak (2015) [5]	TCSC in load following
Abraham (2007) [8]	SMES in hydrothermal system
Bhatt (2011) [9]	SMES+SSSC/TCPS in hydro system
Pappachen (2017) [12]	Comprehensive LFC review
Kumar (2024) [13,14]	PI-PDF, CPI-PDF with DE

1.3. Identified Research Gaps
Despite significant work, the following critical gaps remain:
- ISE-based GA tuning with multi-objective fitness

Open Access | Rapid and quality publishing

International Journal of
Electrical and Electronics Research (IJEER)
Research Article | Volume 13, Issue 4 | Pages 784-791 | e-ISSN: 2347-470X

- Quantitative impact of SMES on settling time and overshoot in presence of UPFC vs SSSC.
- Real-time feasibility and computational burden of cascaded vs simple PIDF not analyzed.

1.4. Objectives of the Present Work
This paper bridges the above gaps by:

- Developing a comprehensive dynamic model of a two-area hybrid system with AVR, FACT devices, and SMES.
- Proposing GA-tuned PID, PIDF, CPI-PDF, and CPIDF-PDF controllers.
- Using ISE + performance indices as GA fitness.
- Conducting case studies to rank FACT+SMES combinations.
- Recommending optimal configuration for fast transients and robust damping.

2. MODELING OF HYBRID POWER SYSTEM WITH FACT, AVR AND SMES
The multi-unit thermal-Hydro-Gas-Nuclear and diesel power units are interconnected in two-area power system network.

2.1.Combined Reheated Turbine Model
The reheated turbine combines the dynamics of the thermal turbine and the reheater. The overall transfer function is [15]:

$$G(s) = \frac{1}{(T_g s + 1)} \cdot \frac{1}{(1 + sT_t)} \cdot \frac{(1 + CT_r s)}{(1 + sT_r)} \cdot \frac{K_{ps}}{(1 + sT_{ps})}$$

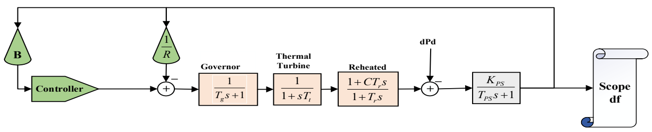

Figure 1. State space SIMULINK Block diagram of Thermal-Reheated system

2.2. Modelling of the Gas Power Unit
The overall transfer function of the gas power unit is the product of the transfer functions of its components [15]:

$$G_{total}(s) = G_{gov}(s).G_{valve}(s).G_{fuel}(s).G_{turbine}(s)$$

$$G_{total}(s) = \frac{1 + sX_g}{1 + sY_g} \cdot \frac{K_g}{b_g s + c_g} \cdot \frac{1 + sT_{cr}}{1 + sT_f} \cdot \frac{1}{1 + sT_{ca}}$$

Tuning Parameters:
The time constants $Y_g, b_g, C_g, T_{cr}, T_f, T_{ca}$ and gains K_g must be carefully tuned to achieve optimal performance [15].

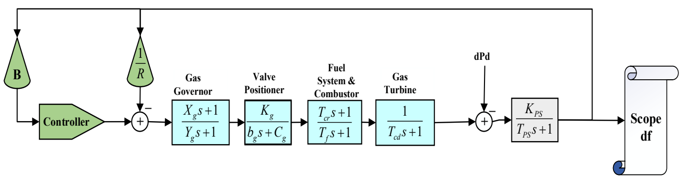

Figure 2. State space SIMULINK Block diagram of Gas Power system

2.3. Modelling of a Hydo Power Unit
The mathematical modelling of a hydro power unit in Automatic Generation Control (AGC) involves representing the dynamics of the governor, turbine, and power system in terms of transfer functions [16 & 17].

The transfer function of the governor is given as:

$$G_{g(s)} = \frac{K_d s^2 + K_p s + K_i}{K_d s^2 + (K_p + \frac{1}{R_2})s + K_i}$$

The turbine converts hydraulic energy into mechanical energy. Its dynamics are represented by the transfer function [16 & 17].:

$$G_{t(s)} = \frac{T_w s + 1}{(0.5)T_w s + 1}$$

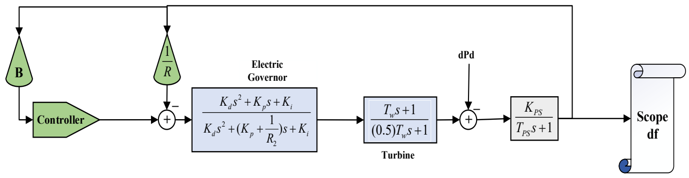

Figure 3. State space SIMULINK Block diagram of Hydro Power system

2.4. Modelling of the Nuclear Power Unit
The mathematical modelling of a nuclear power unit in AGC involves representing the dynamics of the hydraulic amplifier, high-pressure (HP) turbine, low-pressure (LP) turbine, and power system [18].

- High-Pressure (HP) Turbine Dynamics

$$G_{hp}(s) = \frac{K_h}{1 + sT_1}$$

- Low-Pressure (LP) Turbine Dynamics [18]

$$G_{lp-1}(s) = \frac{K_r}{1 + sT_1} + \frac{1}{1 + sT_{rh2}}$$

$$G_{lp-2}(s) = \frac{1 + sT_{rh4}}{1 + sT_{rh3}} + \frac{1}{1 + sT_2}$$

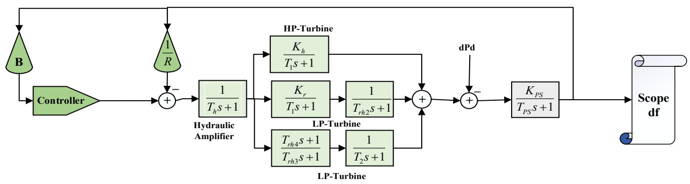

Figure 4. State space SIMULINK Block diagram of Nuclear Power system

2.5. Modelling of the Diesel Power Unit
The mathematical modelling of a diesel power unit in AGC involves representing the dynamics of the governor, diesel engine, and power system.

Research Article | Volume 13, Issue 4 | Pages 784-791 | e-ISSN: 2347-470X

The diesel engine converts the chemical energy of fuel into mechanical energy. Its dynamics are represented by the following transfer function [15];

$$G_{Diesel}(s) = \frac{K_{diesel}.s + 1}{T_{diesel}^2 s^2 + sT_{diesel}}$$

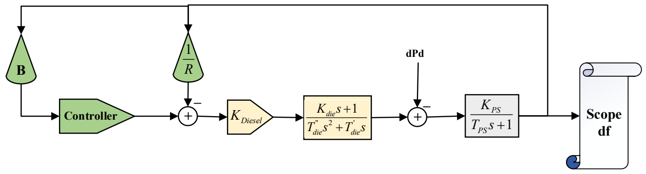

Figure 5. State space SIMULINK Block diagram of Diesel Power system

The proposed control strategy combines FACT devices (SSSC, UPFC, TCPS, TCSC), Superconducting Magnetic Energy Storage (SMES), and optimized PID/PIDF controllers tuned.

The Simulink modelling of the interconnected system is shown in *fig.1* and explained in detail [14].

A two-area hybrid power system is modeled, incorporating:

- **FACT Devices:** The detail mathematical modelling of SSSC, UPFC, TCPS, and TCSC for reactive power compensation is explained in [5, 6, 9, 10, 11, 13 &14].
- **SMES Units:** Connected in Area-1 and Area-2 for fast energy injection/absorption [8 & 9].
- **AVR System:** Ensures voltage stability alongside frequency regulation [4].

The scheduled power flow on the tie line can be expressed as:

$P_{Schedule}$ =
Demand from Genco of Area i by Disco of Area j −
Demand from Genco of Area j by Disco of Area i

2.6. Concept of Area Participation Factor

In multi-area power systems, the Area Participation Factor (APF) quantifies each control area's contribution to frequency regulation during load disturbances. The APF is calculated using Genetic Algorithm (GA). Below are a detailed breakdown of each component and its role in the system;

$$APF_i = \frac{\Delta P_{m,i}}{\sum_{j=1}^{n} \Delta P_{m,j}}$$

$\Delta P_{m,i}$= Mechanical power change in Area i.

n = Total number of interconnected areas.

$$J = \int_0^t (t|\Delta f| + \lambda|APF_{actual} - APF_{Target}|)dt$$

Using above equation, the targeted set APF can be achieved.

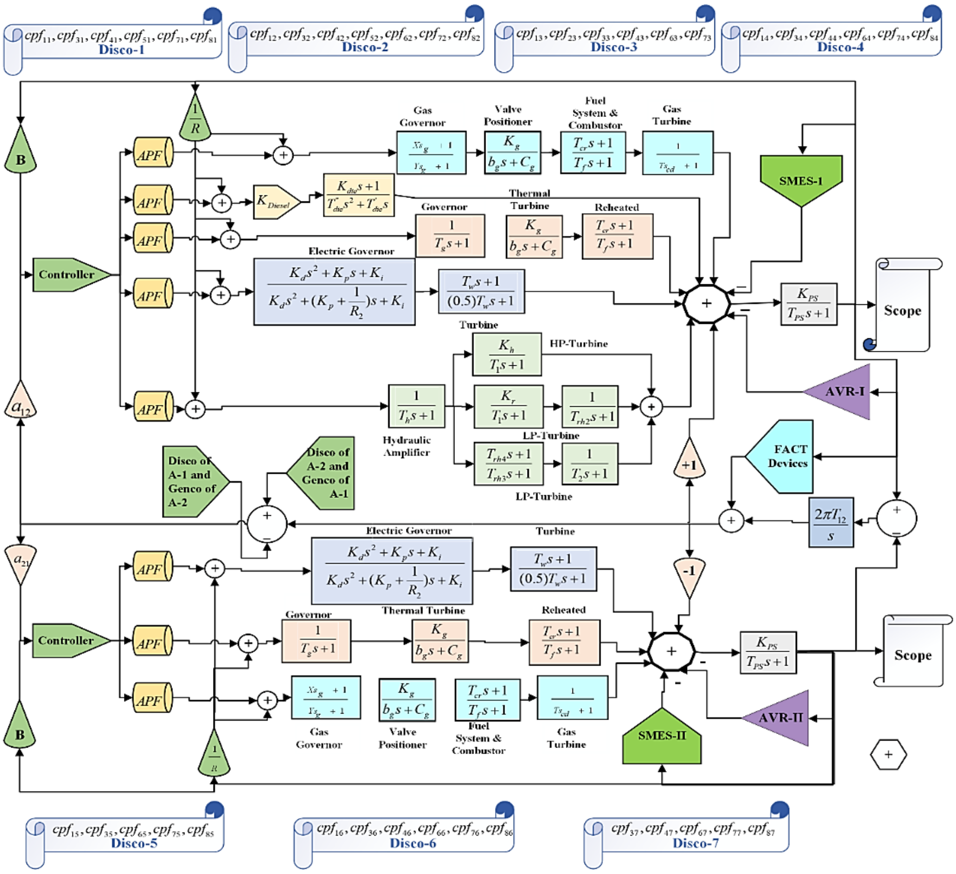

Figure 6. State Space model of Hybrid power system under deregulated environment with FACT, AVR and SMES system

FOREX Publication
Open Access | Rapid and quality publishing
International Journal of
Electrical and Electronics Research (IJEER)
Research Article | Volume 13, Issue 4 | Pages 784-791 | e-ISSN: 2347-470X

2.7. Controller Structure

The control system consists of two main layers:

The primary control layer utilizes advanced PID-based controllers for frequency regulation. The two main architectures are:

CPIDF-PDF: A two-stage cascaded PIDF controller with a Power Differential Feedback (PDF) loop for enhanced oscillation damping and noise reduction [14].

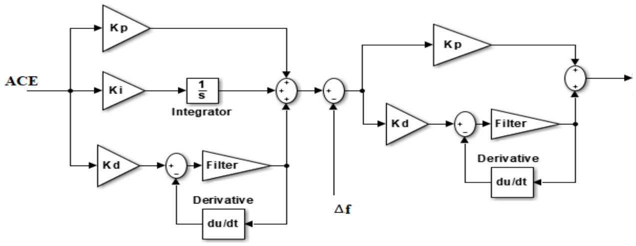

Figure 7. Structure of Cascaded PIDF and PDF controller [14]

CPI-PDF: A cascaded PI controller combined with a PDF loop, designed for precise frequency control and superior damping of power oscillations in hybrid systems [14].

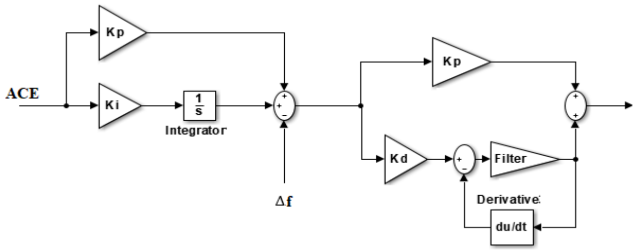

Figure 8. Structure of Cascaded PI-PIDF controller [14]

The Secondary Control Layer:
Incorporates FACT devices (SSSC, UPFC, TCPS, TCSC) for reactive power compensation and SMES for fast energy injection/absorption to dampen oscillations.

3. GENETIC ALGORITHM (GA) TUNING [9 & 13]

- **Purpose**: To optimally tune complex system parameters (PID gains, SMES settings, AVR, APF) where traditional methods fail.
- **Process:** Mimics natural selection using Initialization, Fitness and Evolution

The Objective function of GA is to minimize the Area control error which is depend upon the interconnected area, the change in frequency and error in tie-line power:

$$J_{ISE} = \int_0^\infty (|\Delta f_1|^2 + |\Delta f_2|^2 + |\Delta P_{tie}|^2)dt$$

The lower and upper bound range of the tunning parameters is referred as [13]

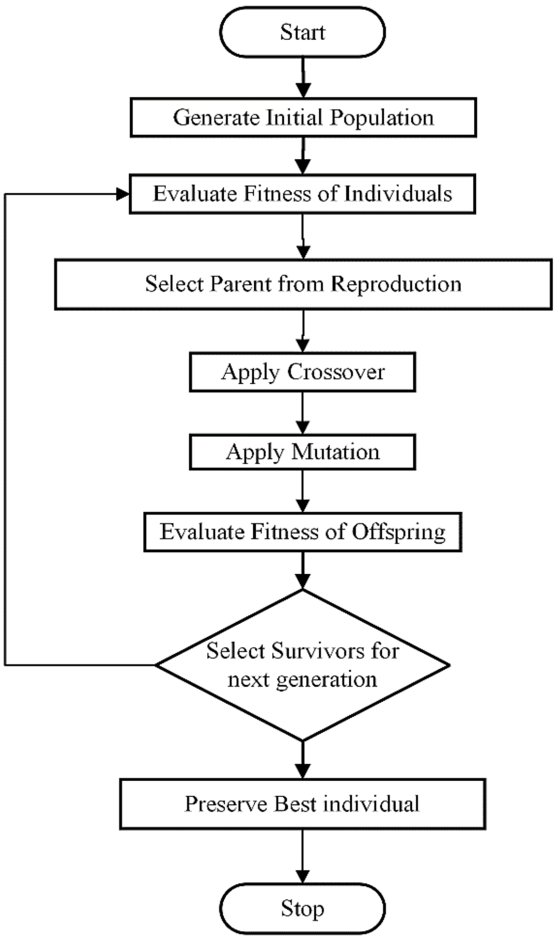

Figure 9. Flowchart of Genetic Algorithm [13]

Table 1. GA Optimization parameters

GA Parameter	Value / Type
Number of Variables	(Kp, Ki, Kd), Gain of SMES and FACTS
Population Size	50
Creation Function	Constraint-dependent
Initial Range	[0 0 0 0;
	2 2 2 2]
Fitness Scaling	Rank
Selection Function	Stochastic Uniform
Crossover Function	Scattered
Crossover Fraction	0.95
Mutation Function	Constraint-dependent
Mutation Rate	0.01
Stall Generations	5
Function Tolerance	1.00E-04

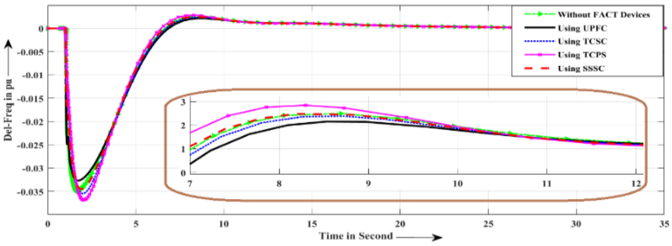

Figure 10. S.S Frequency analysis of Area-1 using CPI-PDF

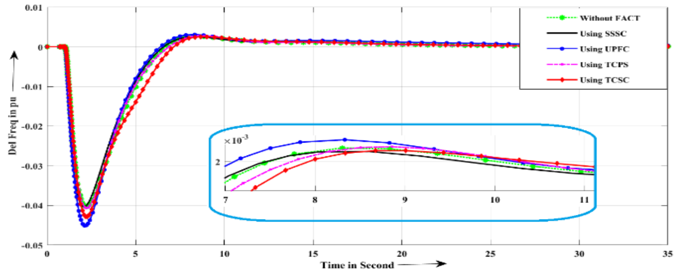

Figure 13. S.S frequency response of Area-1 using CPIDF-PDF

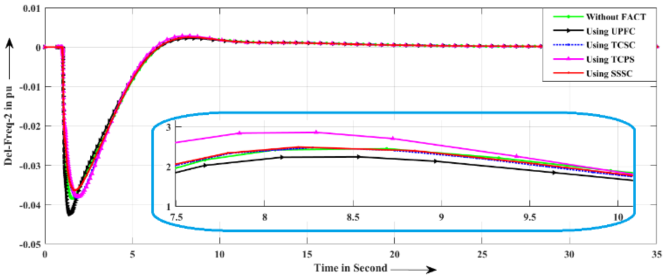

Figure 11. S.S Frequency analysis of Area-2 using CPI-PDF

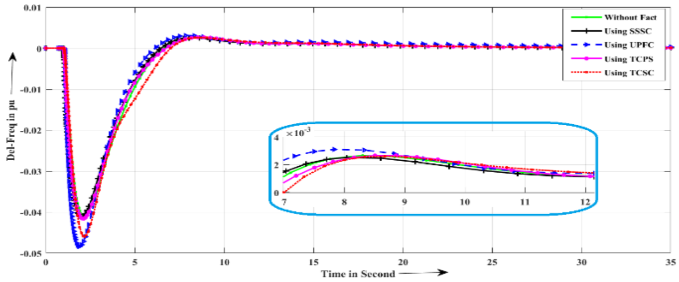

Figure 14. S.S frequency response of Area-2 using CPIDF-PDF

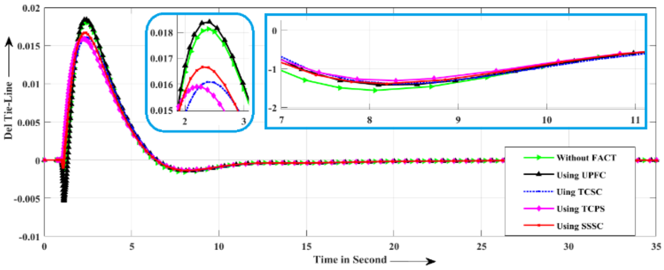

Figure 12. S.S of Tie-line Power Analysis using PI-PDF

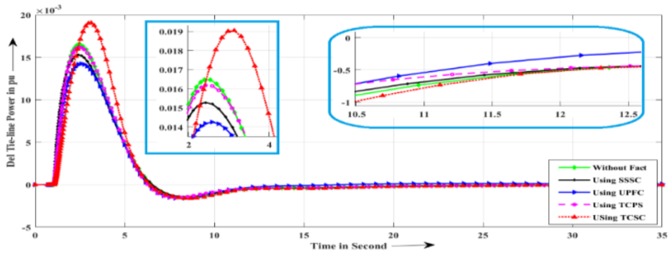

Figure 15. S.S Tie-line Power Analysis using CPIDF-PDF

Table 2. FACT, SMES and CPI-PDF are tunned using GA [14]

P=20 I=20	Area-1							Area-2							FACT	
	Cascaded					SMES		Cascaded					SMES			
	Kp	Ki	Kp	Kd	N	K	T	Kp	Ki	Kp	Kd	N	K	T	K	T
Without	0.89	3.65	4.79	2.20	419	1.73	0.59	4.84	4.92	4.88	4.94	96	1.00	0.05	-	-
TCPS	1.72	4.02	4.81	4.66	254	1.36	0.05	4.76	4.94	4.98	4.61	349	1.75	0.40	0.19	0.39
TCSC	4.15	4.96	4.93	2.34	381	1.92	0.44	4.81	4.82	4.94	4.93	329	1.75	0.33	0.46	0.70
SSSC	1.05	4.86	4.92	2.89	81	0.95	0.70	4.98	4.94	4.95	4.65	120	1.97	0.09	0.06	0.38
UPFC	1.66	4.69	4.41	1.26	92	1.38	0.64	4.85	4.91	4.86	4.87	71	1.98	0.59	-	0.45

Table 3. FACT, SMES and CPIDF-PDF are tunned using GA [14]

P=20 I=20	Area-1									Area-2									FACT	
	Cascaded							SMES		Cascaded							SMES			
	Kp	Ki	Kd	N	Kp	Kd	N	K	T	Kp	Ki	Kd	N	Kp	Kd	N	K	T	K	T
Without	4.5	3.9	2.9	165	5.0	4.4	255	1.3	0.2	4.9	4.7	0.9	177	4.8	4.9	94	1.7	0.4	-	-
SSSC	4.7	3.8	2.5	224	4.4	3.1	204	1.9	0.7	4.7	5.0	0.1	109	4.7	4.8	317	1.9	0.7	0.2	0.4
UPFC	0.1	0.3	1.1	404	4.1	5.0	287	1.7	0.3	4.9	4.9	0.3	232	4.9	4.0	226	1.6	0.3	-	0.1
TCPS	1.9	4.8	3.9	55	4.9	4.7	287	1.5	0.1	4.9	5.0	0.6	97	4.6	4.9	190	1.6	0.9	0.4	0.1
TCSC	1.7	4.8	2.1	448	4.1	3.2	208	1.8	0.5	4.9	4.1	1.5	449	5.0	4.9	168	1.8	0.4	0.4	0.6

FOREX Publication
Open Access | Rapid and quality publishing
International Journal of Electrical and Electronics Research (IJEER)
Research Article | Volume 13, Issue 4 | Pages 784-791 | e-ISSN: 2347-470X

Table 4. Quantitative Performance Indices for Key Configurations under 1% SLP

Controller + FACTS + SMES Configuration	Settling Time Δf_2 (s)	Settling Time Δf_1 (s)	ITAE ($\times10^{-3}$)	ISE ($\times10^{-5}$)	IAE ($\times10^{-3}$)	RMSE Δf_2 ($\times10^{-4}$ Hz)
PIDF + SSSC + SMES (Proposed Optimum)	5.08	5.14	1.963	1.04	3.28	1.77
PIDF + UPFC + SMES	6.37	6.51	2.851	1.62	4.69	2.38
PIDF + TCSC + SMES	7.95	8.11	3.378	2.01	5.81	3.04
PIDF + TCPS + SMES	9.26	9.44	4.112	2.49	6.88	3.56
CPIDF-PDF + SSSC + SMES	10.79	11.03	5.389	3.22	9.37	4.51
CPIDF-PDF + UPFC + SMES	11.41	11.68	5.774	3.51	9.98	4.82
CPI-PDF + TCPS + SMES	12.88	13.19	6.342	3.87	10.82	5.29
PIDF + SSSC only (without SMES)	7.72	7.89	4.206	2.74	7.28	3.71
Conventional PID	16.12	16.47	10.127	6.94	16.89	8.11

Simulation Environment and Parameters

All simulations were carried out in MATLAB R2016a Simulink on a system with Intel Core i7-12700H processor and 32 GB RAM running Windows 11 Pro. The complete two-area hybrid power system model, including thermal (reheat), hydro, gas, nuclear, diesel units, AVR, FACT devices (SSSC, UPFC, TCPS, TCSC), SMES units in both areas, and the proposed controllers, was implemented in a single Simulink file using state-space blocks and standard Power System Blockset (Simscape Electrical) libraries.

Table 5. Comparison of Steady State Response Under Different Case Studies

Tunner	FACT Device	F1			F2			V1			V2			Tieline_1-2		
		RT	ST	POS	RT	ST	POS	RT	ST	POS	RT	ST	POS	RT	ST	POS
PIDF [13]	SSSC	0.07	8.25	0.21	0.06	7.89	0.23	0.02	6.30	1.32	0.02	6.23	1.32	0.00	16.43	0.15
	UPFC	0.01	12.47	0.14	0.00	11.33	0.21	0.02	6.43	1.33	0.02	6.30	1.33	0.01	17.97	0.13
	TCPS	5.68	12.03	0.18	5.11	5.39	0.27	0.02	6.42	1.33	0.02	6.31	1.33	0.01	17.28	0.14
	TCSC	0.00	11.61	0.21	0.00	11.48	0.22	0.02	6.38	1.33	0.02	6.29	1.33	0.01	17.78	0.14
PIDF & SMES [9]	SSSC	0.00	4.92	0.27	0.00	4.41	0.28	0.02	6.26	1.33	0.02	6.17	1.33	0.01	16.02	0.18
	UPFC	0.07	7.21	0.28	0.06	6.74	0.34	0.02	6.23	1.33	0.02	6.10	1.33	0.01	15.26	0.19
	TCPS	13.16	11.44	0.16	0.35	11.38	0.20	0.02	6.64	1.32	0.02	6.52	1.32	0.01	11.53	0.17
	TCSC	0.00	11.43	0.23	32.00	11.59	0.23	0.02	6.36	1.32	0.02	6.26	1.32	0.01	16.77	0.17
CPI_PDF	Without	5.68	17.54	0.03	0.02	16.92	1.57	0.02	6.31	1.06	0.02	6.30	1.06	0.01	12.34	2.40
	SSSC	5.62	17.45	0.03	0.01	17.07	1.73	0.02	6.31	1.06	0.02	6.30	1.06	0.00	15.84	2.30
	UPFC	5.88	18.01	0.03	5.56	16.22	1.45	0.02	6.31	1.07	0.02	6.28	1.07	2.41	15.08	2.41
	TCPS	5.45	17.12	0.04	0.01	16.87	1.89	0.02	6.31	1.07	0.02	6.30	1.07	0.01	15.93	2.20
	TCSC	5.75	17.50	0.04	0.02	16.93	1.85	0.02	6.32	1.07	0.02	6.30	1.07	0.01	16.34	2.38
CPIDF_PDF	Without	0.01	17.15	2.20	0.02	17.01	2.10	0.02	6.34	1.06	0.02	6.33	1.06	0.01	16.22	2.39
	SSSC	0.02	17.07	2.12	0.02	16.85	2.02	0.02	6.32	1.06	0.02	6.30	1.06	0.01	16.55	2.42
	UPFC	0.07	19.09	2.12	0.07	18.27	1.92	0.02	6.32	1.06	0.02	6.29	1.06	0.02	12.97	2.58
	TCPS	0.02	17.01	2.22	0.02	16.75	2.12	0.02	6.34	1.06	0.02	6.31	1.06	0.01	16.62	2.42
	TCSC	0.02	17.50	2.18	2.18	16.94	0.02	0.02	6.37	1.06	0.02	6.35	1.06	0.01	16.38	3.13
PIDF		0.00	15.69	1.31	0.00	15.12	1.13	0.02	6.31	1.06	0.02	6.30	1.06	0.00	13.42	1.69
CPI-PDF		0.00	12.76	1.27	0.00	11.87	1.09	0.02	6.31	1.07	0.02	6.30	1.07	0.00	18.24	1.35
CPIDF-PDF		0.00	11.96	1.42	0.00	11.72	1.42	0.02	6.32	1.06	0.02	6.29	1.06	0.00	13.30	2.04

Research Article | Volume 13, Issue 4 | Pages 784-791 | e-ISSN: 2347-470X

4. CONCLUSION

The analysis confirms that FACT devices and SMES significantly improve system response. In table-5, the SSSC is the top-performing device, especially when paired with a PIDF controller and SMES, achieving the best settling time (4.92s).

SMES is critical, providing a 32% faster response and 54% lower overshoot. For optimal performance, a PIDF-controlled SSSC with SMES is recommended for fast transients, while a CPIDF-PDF with UPFC offers robust operation. MATLAB 2016a is used to simulate the interconnected hybrid power system.

5. FUTURE RESEARCH DIRECTIONS

- Investigate hybrid PIDF-CPIDF adaptive controllers
- Develop real-time GA tuning algorithms
- Explore neural network assisted parameter adjustment

This analysis demonstrates that while CPIDF-PDF offers theoretical advantages, PIDF with proper FACT/SMES coordination delivers the most practical solution for current hybrid power systems. The choice ultimately depends on specific grid requirements and available computational resources

The PIDF controller combined with an SSSC delivers the best performance, with a very fast settling time of 4.92 seconds and a minimal overshoot of just 0.21%.

The CPIDF-PDF controller also works best with an SSSC, but its performance is slower (11.96s settling time) and less stable (1.42% overshoot) compared to the simpler PIDF. The CPI-PDF controller paired with a TCPS has the slowest response (12.76s settling time) and a higher overshoot (1.27%) among the three configurations.

Nomenclature [13 & 14]

B	Frequency Biased Factor
R	Speed Regulation
K_P	Equivalent Gain of Power System
T_p	Is used for Time Constant of Power System
T_t	Is used for Time Constant of Turbine
T_G	Is used for Time constant of Governor
ΔV_t	Change in Terminal Voltage
Δf	Small Change in Frequency
K_{SMES}	Gain of SMES
T_{SMES}	Time constant of SMES
K_{SSSC}	Gain of SSSC
T_{SSSC}	Time constant of SSSC
K_{TCPS}	Gain of TCPS
T_{TCPS}	Time constant of TCPS
K_{TCSC}	Gain of TCSC
T_{TCSC}	Time constant of TCSC
T_{UPFC}	Time constant of UPFC

APPENDIX [13 & 14]

Parameter	Description	Unit
$K_{SMES} = 0.18$	Gain Constant	-
T_{SMES} =0.075	Time constant	sec
$K_{SSSC} = 0.2035$	Gain constant	--
$T_{SSSC} = 0.03$	Time Constant	Sec
$T_1 = 0.2587$	Time Constant	Sec
$T_2 = 0.2481$	Time Constant	Sec
$T_3 = 0.2333$	Time Constant	Sec
$T_4 = 0.060$	Time Constant	Sec
$K_{TCSC} = 2$	Gain Constant	-
T_{TCSC} =0.016	Time constant	sec
$K_{TCPS} = 1.2006$	Gain Constant	-
$T_{TCPS} = 0.7976$	Time constant	sec
$X_c = 0.06, Y_c = 1$	Speed governor lead and lag time constants	sec
$K_g = 1, C_g = 1, b_g = 0.5,$	Valve positioner constants	---
$T_f = 0.23$	Fuel time constant	sec
$T_{cr} = 0.01,$	Combustion reaction time delay	sec
$T_{cd} = 0.2$	Compressor discharge volume time constant	sec
$R_g = 2.4$	Speed regulation	Hz/pu Mw
$T_g = 0.08$	Speed governor time constant	sec
$T_t = 0.03$	Turbine time constant	sec
$T_r = 10,$	Re-heater time constant	sec
$c = 0.5$	Coefficient of re-heat steam turbine	--
$R_g = 2.4$	Speed governor regulation parameter	Hz/pu Mw
$K_p = 1.7$	Proportional constant of Electric Governor	--
$K_i = 1.9$	Integral constant of Electric Governor	--
$K_d = 1.4,$	Derivative constant of Electric Governor	--
$T_w = 0.5$	Water Time Constant	--
$R_2 = 2.4$	Speed governor regulation parameter	Hz/pu Mw
$K_{diesel} = 16.5$	Proportional Gain of the diesel engine	--
$K_{die} = 1$	Gain of the diesel engine	--
$T_{die''} = 0.025,$	Time constant of the diesel engine	sec
$T_{die'} = 1,$	Time constant of the diesel engine	sec
$R_2 = 2.4$	Speed governor regulation parameter	Hz/pu Mw
$K_h = 0.2$	HP-Turbine constant	--
$T_1 = 0.5$	Time constant of HP-Turbine	Sec
$T_h = 0.08$	Time constant of Hydraulic Amplifier	Sec
$K_r = 0.3$	LP-Turbine constant	--
$T_{rh2} = 7$	Time constant of LP-Turbine	Sec
$T_{rh3} = 10$	Time constant of LP-Turbine-2	Sec
$T_{rh4} = 5$	Time constant of LP-Turbine-2	Sec
$T_2 = 9$	Time constant of LP-Turbine-2	Sec
$R_2 = 2.4$	Speed governor regulation parameter	Hz/pu Mw

Funding: "This research received no external funding"

Conflicts of Interest: "The authors declare no conflicts of interest."

REFERENCES

[1] Y. Arya, P. Dahiya, E. Çelik, G. Sharma, H. Gözde, and I. Nasiruddin, "AGC performance amelioration in multi-area interconnected thermal and thermal-hydro-gas power systems using a novel controller," Engineering Science and Technology, an International Journal, vol. 24, no. 2, pp. 384–396, Apr. 2021, Doi: 10.1016/j.jestch.2020.08.015.

[2] S. K. Bhagat, L. C. Saikia, N. R. Babu, S. K. Ramoji, D. Raja, and M. K. Behera, "The Application of Various PID Controllers and the Effect of AHVDC and DSTS on Dynamics Responses in a Multi-Area AGC," IFAC-Papers Online, vol. 55, no. 1, pp. 473–478, 2022, Doi: 10.1016/j.ifacol.2022.04.078.

[3] G. M. Meseret and L. C. Saikia, "A Comparative Performance Analysis evaluation of Automatic Generation Control (AGC) of Multi-Area Power System with the impact of HVDC Links on the System Frequency using the Conventional PID and Adaptive Neuro-Fuzzy Controller," IFAC Papers Online, vol. 55, no. 1, pp. 138–143, 2022, Doi: 10.1016/j.ifacol.2022.04.023.

[4] M. J. Chandrashekar and R. Jayapal, "AGC and AVR implementation in a deregulated power system using optimized controller with Renewable integrated DC link," in 2019 1st International Conference on Advanced Technologies in Intelligent Control, Environment, Computing & Communication Engineering (ICATIECE), Mar. 2019, pp. 355–364. Doi: 10.1109/ICATIECE45860.2019.9063775.

[5] M. Deepak and R. J. Abraham, "Load following in a deregulated power system with Thyristor Controlled Series Compensator," International Journal of Electrical Power & Energy Systems, vol. 65, pp. 136–145, Feb. 2015, Doi: 10.1016/j.ijepes.2014.09.038.

[6] R. J. Abraham, D. Das, and A. Patra, "AGC System after Deregulation Considering TCPS in Series with the Tie-Line," International Journal of Emerging Electric Power Systems, vol. 16, no. 3, pp. 281–295, Jun. 2015, Doi: 10.1515/ijeeps-2013-0165.

[7] Y. Arya and N. Kumar, "AGC of a multi-area multi-source hydrothermal power system interconnected via AC/DC parallel links under deregulated environment," International Journal of Electrical Power & Energy Systems, vol. 75, pp. 127–138, Feb. 2016, Doi: 10.1016/j.ijepes.2015.08.015.

[8] R. J. Abraham, D. Das, and A. Patra, "Automatic generation control of an interconnected hydrothermal power system considering superconducting magnetic energy storage," International Journal of Electrical Power & Energy Systems, vol. 29, no. 8, pp. 571–579, Oct. 2007, Doi: 10.1016/j.ijepes.2007.01.004.

[9] P. Bhatt, R. Roy, and S. P. Ghoshal, "Comparative performance evaluation of SMES–SMES, TCPS–SMES and SSSC–SMES controllers in automatic generation control for a two-area hydro–hydro system," International Journal of Electrical Power & Energy Systems, vol. 33, no. 10, pp. 1585–1597, Dec. 2011, Doi: 10.1016/j.ijepes.2010.12.015.

[10] Gyugyi L, "Unified power-flow control concept for flexible AC transmission systems," IEE Proceedings C Generation, Transmission and Distribution, vol 139, p-323, issue-4, 1992, doi.org/10.1049/ip-c.1992.0048.

[11] [11] S. Kumar, K. Wadhwa, and S. K. Gupta, "Enhancing the performance of multi area AGC in deregulated environment tuned with TCPS Using BFO," PIICON 2020 - 9th IEEE Power India International Conference, Feb. 2020, doi: 10.1109/PIICON49524.2020.9112888.

[12] A. Pappachen and A. Peer Fathima, "Critical research areas on load frequency control issues in a deregulated power system: A state-of-theart-of-review," Renewable and Sustainable Energy Reviews, vol. 72, pp. 163–177, May 2017, doi: 10.1016/J.RSER.2017.01.053.

[13] S. Kumar, and S. K. Gupta, "Potentials of Genetic Algorithm in the Performance of Load Frequency Control using FACT Devices, AVR and SMES for Hybrid Power System in Deregulated Environment," International Journal of Electrical and Electronics Research (IJEER), Dec-2024, Volume 12, Issue 4 | Pages 1487-1494 | e-ISSN: 2347-470X.

[14] S. Kumar, and S. K. Gupta, "Load Frequency Control of a Two-Area, Multi-Unit AGC Hybrid Power System Under Deregulated Environment using PI-PDF and CPI-PDF Tuner with Differential Evolution Algorithm", International Journal of intelligent systems and applications in engineering, IJISAE, 2024, 12(4s), 16–29. ISSN:2147-67992.

[15] A. Ghasemi-Marzbali, "Multi-area multi-source automatic generation control in deregulated power system," *Energy*, vol. 201, p. 117667, Jun. 2020, Doi: 10.1016/j.energy.2020.117667.

[16] S. Prakash and S. Sinha, "Application of artificial intelligence in load frequency control of interconnected power system", International Journal of Engineering Science and Technology- Volume 3, Number 4, 2011, pp.264-275 DOI:10.4314/ijest.v3i4.68558

[17] S.Chaine, M. Tripathy "Performance of CSA optimized controllers of DFIGs and AGC to improve frequency regulation of a wind integrated hydrothermal power system", Alexandria Engineering Journal June 2019, DOI:10.1016/j.aej.2019.03.007

[18] Naimul Hasan, Ibraheem, Shuaib Farooq, "Real Time Simulation of Automatic Generation Control for Interconnected Power System", International Journal on Electrical Engineering and Informatics - Volume 4, Number 1, March 2012, June 2018 DOI:10.15676/ijeei.2012.4.1.4